ICIC Express Letters
Volume **12**, Number **7**, July **2018**

ICIC International ©2018 ISSN 1881-803X
pp. **671–679**

DECOUPLING CONTROL STRATEGY FOR DISCRETE SLIDING MODE CURRENT COMPENSATION OF HIGH SPEED IPMSM

Yan Dong[1], Ruizhi Xin[1], Hao Zhang[1] and Lingling Li[2]

[1]Department of New Energy Science and Engineering
[2]Department of Electrical Engineering and Automation
Hebei University of Technology
No. 5340, Xiping Road, Beichen District, Tianjin 300401, P. R. China
dongyan73@hebut.edu.cn

Received January 2018; accepted April 2018

Abstract. *In the high-speed interior permanent magnet synchronous motor (IPMSM) vector control system, the robustness of the system is always decreased due to the problems which exist in the current decoupling process. It is caused by those factors: the speed-dependent cross-coupling terms due to coordinate transformation, the presence of control response delays in digital systems, and the sensitivity of parameter changes for traditional decoupling strategies. In this paper, based on the discrete model of motor, the direct design method is proposed to design the decoupling controller with discrete sliding mode current compensation, which not only ensures the decoupling performance of the system, but also increases the adaptability to the motor parameters. Simulation and experimental results demonstrate the effectiveness of the proposed approach.*
Keywords: High-speed interior permanent magnet synchronous motor, Direct design method, Current loop decoupling, Discrete mathematical model, Sliding mode current compensation control

1. **Introduction.** Because of the high efficiency and high inertia ratio characteristics, IPMSM is widely used in electric vehicles, heavy industrial machinery and other industrial occasions [1]. High-speed IPMSM gets more attention because of its smaller, lighter weight, higher power density. However, the maximum fundamental frequency makes the control more difficult. On the one hand, the transformation of electric variables to a synchronous reference frame creates cross-coupling that is proportional to the maximum fundamental frequency. As a result, the performance of the current regulator has been shown to degrade as the maximum fundamental frequency increases [2]. On the other hand, the use of pulse width modulation (PWM) to control the inverter forces additional delays between the sampling of signals and the application of the control response will complicate the controller design and decrease the system's overall stability [3]. Thirdly, discretization of the current controllers designed in the continuous-time domain degrades the robustness of the closed-loop system because of errors introduced by discretization method approximation [4]. In order to solve the problem, voltage feed forward decoupling, state feedback decoupling, internal model control and other methods are adopted. However, they all are first designed in the continuous-time domain and then discretized for the digital implementation using [5]. This approach is well understood and works well in most applications. However, the ratio between the sampling frequency and the maximum fundamental frequency should be more than 10 [4].

A. Altomare et al. established a discrete model of three-phase inverter-driven permanent magnet synchronous motor with delay in the discrete domain, and proposed a new type of direct discrete current controller which uses the zero-pole cancellation method in

DOI: 10.24507/icicel.12.07.671

[6], and it solves the problem of current coupling caused by digital control and time delay. The system performance is ideal when no parameter changes and external disturbances occur. However, the inductances L_d and L_q are nonlinear functions of both current components i_d and i_q [7]. If the parameters change, it will lead to the system closed-loop zero-pole cannot be cancelled well, and the damping factor will be deteriorated at the same time.

M. Comanescu et al. proposed a new approach for decoupled current control in [8]. The cross-coupling terms of the d-q current dynamics were treated as unknown disturbances. Integral-sliding-mode (*ISM*) controllers are used to reject these disturbances. However, as the speed increases, the proportion of the coupling voltage is increasing, and it will require high-gain to make the system stable. However, the high-gain will lead the output voltage to becoming high frequency switch which will bring high frequency noise and buffeting.

A discrete sliding mode current compensation controller is proposed in this paper which is based on the accurate discrete mathematical model of the motor. This control strategy uses the direct discrete controller to decouple the ideal motor model, and uses the discrete sliding mode control to improve the system robustness for the parameter variations and external disturbances in the whole process of motion. Simulation and experimental results are provided to compare the performance, stability, and robustness of the current regulators analyzed.

2. Discrete Mathematical Model of High-Speed Permanent Magnet Motor.

When the IPMSM is running at the high-speed range, the resistive voltage drop can be ignored. The IPMSM model in the α-β stationary reference frame can be described by the following voltage equation:

$$u_{\alpha\beta} = \frac{d\psi_{\alpha\beta}}{dt} \tag{1}$$

where $u_{\alpha\beta}$ are the $\alpha\beta$ stator voltage; $\psi_{\alpha\beta}$ is the stator flux.

In the α-β stationary reference frame, the transfer function of (1) can be expressed as:

$$G_p(s) = \frac{\psi_{\alpha\beta}(s)}{u_{\alpha\beta}(s)} = \frac{1}{s} \tag{2}$$

Ignore the harmonic, the inverter can be treated as an ideal zero-order hold:

$$H(s) = \frac{1 - e^{-sT_s}}{s} \tag{3}$$

where T_s is the sampling period; s is continuous domain.

Based on the discrete control theory, the control object and the zero-order hold are regarded as a generalized control object and then can be discretized. The discrete model of IPMSM is shown in Equation (4), which is driven by the three-phase inverter in the stationary coordinate system of (2) and (3).

$$G_{\alpha\beta}(z) = \frac{\psi_{\alpha\beta}(z)}{u_{\alpha\beta}(z)} = Z\{H(s)G_p(s)\} = \frac{T_s}{z-1} \tag{4}$$

Since the PWM duty cycle command is calculated at the k sampling period, and it is usually executed at $k+1$ sampling period, the digital control system usually has the one-ample period delay. The delay function is:

$$D(z) = \left(ze^{j\omega_e T_s}\right)^{-1} \tag{5}$$

where ω_e is the electrical angular speed; z is discrete domain.

Considering the digital delay, the exact discrete model of the three-phase inverter-driven permanent magnet synchronous motor can be obtained by Equations (4) and (5):

$$G_{dq\_d}(z) = \frac{T_s}{ze^{j\omega_e T_s}\left(ze^{j\omega_e T_s} - 1\right)} \tag{6}$$

3. **Design of Current Decoupling Controller.** In this paper the main controller uses a control strategy proposed by A. Altomare et al. in [6]. However, in the actual situation, the control system will be affected by parameters such as parameter changes and external disturbances. Therefore, a discrete sliding mode current compensation decoupling controller is designed to overcome the shortcomings of the main controller, suppress the interference and improve robustness of the system.

3.1. **Discrete current decoupling controller of direct design method.** Discretization of the current controllers designed in the continuous-time domain degrades the robustness of the closed-loop system because of errors introduced by discretization method approximation. So the direct design method is used to obtain the discrete current regulator in the synchronous rotating coordinate system [6]:

$$G_c(z) = \frac{u_{dq}}{e_{dq}} = \frac{k\left(ze^{j\omega_e T_s}\left(ze^{j\omega_e T_s} - 1\right)\right)}{T_s(z-1)} \tag{7}$$

where $e_{dq} = \psi^*_{dq} - \psi_{dq}$ is the flux error complex vector and k is the controller gain, whose value determines the flux dynamics.

By using (6) and (7), the closed-loop discrete-time transfer function can be expressed:

$$G_o(z) = \frac{G_c(z)G_{dq\_d}(z)}{1 + G_c(z)G_{dq\_d}(z)} = \frac{k}{z^2 - z + k} \tag{8}$$

The root locus of G_o for positive k gains is reported in Figure 1. Closed-loop poles obtained with k in (8) equal to 0, 0.25, 0.35, 1 are evidenced with position 1, 2, 3, 4 at Figure 1. The closed-loop poles are real with gains up to 0.25. A damping equal to 0.707 is reached with $k = 0.35$. Evidently, the root locus is not influenced by the motor fundamental frequency. In the synchronous rotating coordinate, flux can be described as:

$$\psi_{dq}(z) = L_d i_d + \psi_f + jL_q i_q \tag{9}$$

Substituting (9) in (7) gives the following transfer function:

$$u_{dq}(z) = \left[L_d\left(i^*_d - i_d\right) + jL_q\left(i^*_q - i_q\right)\right]\frac{k\left(ze^{j\omega_e T_s}\left(ze^{j\omega_e T_s} - 1\right)\right)}{T_s(z-1)} \tag{10}$$

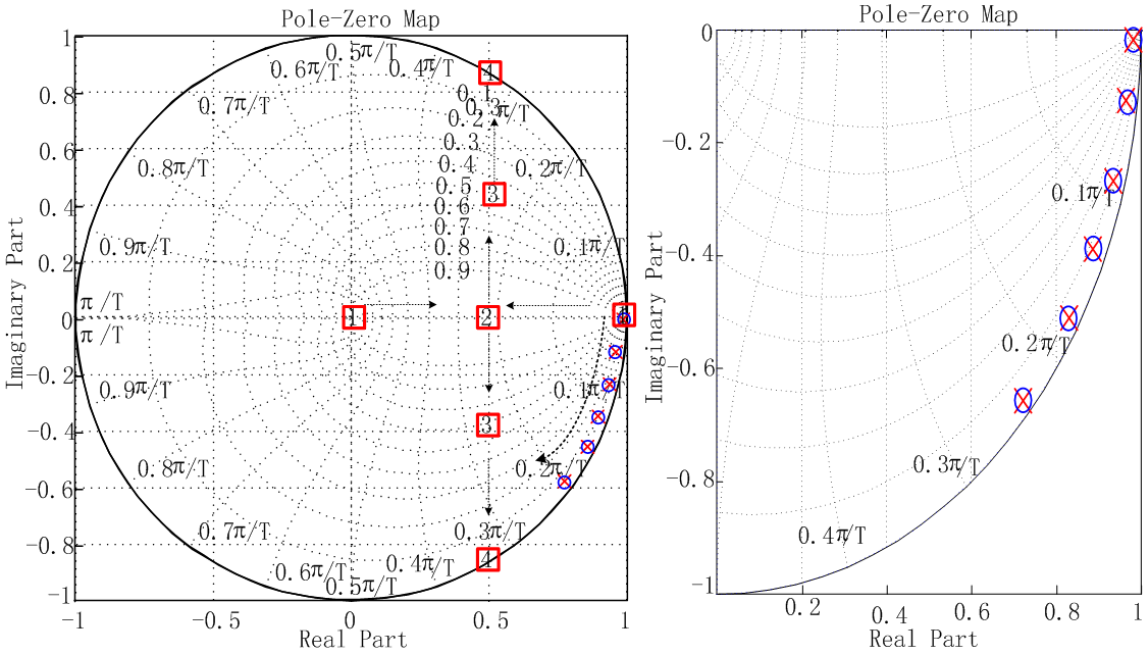

FIGURE 1. Pole-zero map of control system

According to (10), the current regulator block diagram can be got as shown in Figure 2. Ideally, assuming that the motor parameters are accurate, the real current will be same as the ideal current. At this time, the voltage and current can be defined as: $\left[i_d^s, i_q^s\right]^T$, $\left[u_d^s, u_q^s\right]^T$, the motor equation can be written as (11) in d- and q-axes reference frame, and Figure 3 illustrates its structure.

$$\begin{cases} u_{dk}^s = R_s i_{dk}^s + L_d \dfrac{i_{dk+1}^s - i_{dk}^s}{T_s} - \omega_e L_q i_{qk}^s \\ u_{qk}^s = R_s i_{qk}^s + L_q \dfrac{i_{qk+1}^s - i_{qk}^s}{T_s} + \omega_e L_d i_{dk}^s + \omega_e \psi_f \end{cases} \tag{11}$$

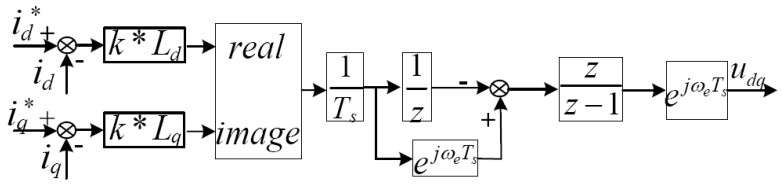

FIGURE 2. Discrete current regulator schematic based on direct design

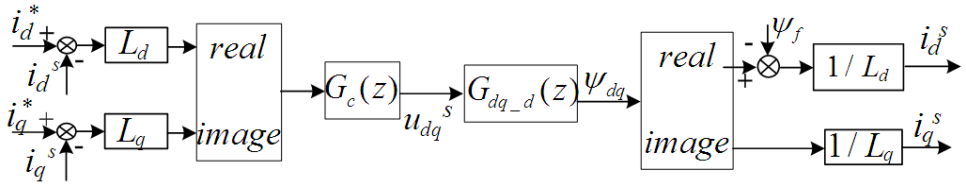

FIGURE 3. Discrete current control system based on direct design

This is the equivalent current control law where the controller gains k_d and k_q have to satisfy the relation $k = k_d/L_q = k_q/L_q$ to guarantee the same dynamic behavior of the current components. However, the inductances L_d and L_q are nonlinear functions of both current components i_d and i_q. If the parameters change, it will lead to the system closed-loop zero-pole cannot be cancelled well, and will deteriorate the damping factor at the same time. Meanwhile, the controller is also less resistant to interference, although it can be increased by increasing the proportional gain, but it will cause the system to oscillate in the dynamic process.

3.2. **Discrete slide mode current compensation decoupling control.** Consider the parameter changes and external disturbances, the motor model can be equivalent to (12):

$$\begin{cases} i_{dk+1} = i_{dk} + \dfrac{T_s}{L_d}\left(L_q \omega_e i_{qk} + u_{dk} - h_d(x,k)\right) \\ i_{qk+1} = i_{qk} + \dfrac{T_s}{L_q}\left(u_{qk} - L_d \omega_e i_{dk} - \psi_f \omega_e - h_q(x,k)\right) \end{cases} \tag{12}$$

While

$$\begin{cases} h_d(x,k) = \Delta L_d i_{dk} - \Delta L_q i_{qk} \omega_e + \varepsilon_d \\ h_q(x,k) = \Delta L_q i_{qk} + \Delta L_d i_{dk} \omega_e + \Delta \psi_f \omega_e + \varepsilon_q \end{cases}$$

where $h_d(x,k)$ and $h_q(x,k)$ are the q- and d-axes disturbance; ΔL_d is d-axis offset; ΔL_q is q-axis offset; $\Delta \psi_f$ is ψ_f offset; ε_d and ε_q are no equivalent of the modeling part.

Discrete sliding mode control (*D-SMC*) proposed in this paper is improved on the original decoupling control strategy, in order to suppress parameter perturbation and external disturbance. Because the sliding mode control does not have the robustness in the approaching stage, the entire trajectory should be ensured on the sliding mode, so the

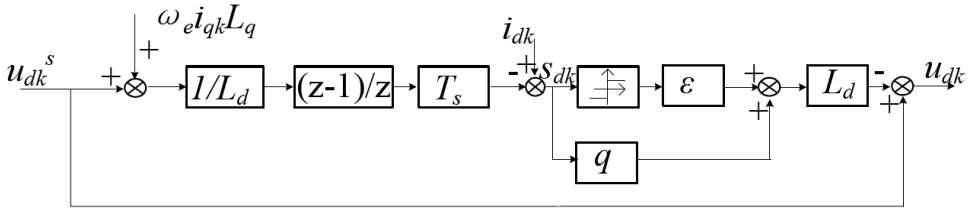

FIGURE 4. SMC diagram of d-axis current

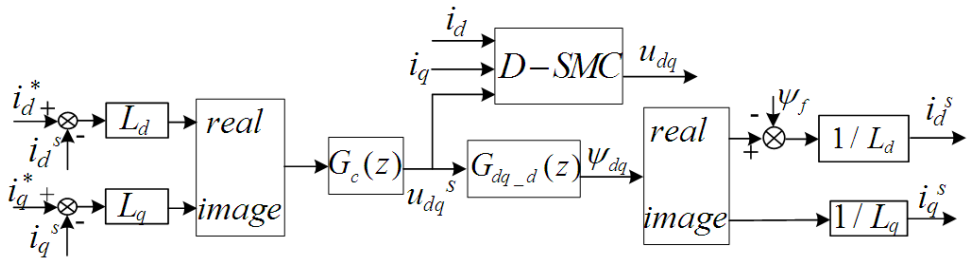

FIGURE 5. SMC control based on direct discrete current control

d-axes sliding surface and control law can be got. The d-axes control schematic is shown in Figure 4. For the d-axes, the sliding surfaces are designed as

$$\begin{cases} s_{dk} = i_{dk} - z_{dk} \\ \dfrac{z_{dk+1} - z_{dk}}{T_s} = \dfrac{u_{dk}^s + \omega_e L_q i_{qk}}{L_d} \\ z_d(0) = 0 \end{cases} \tag{13}$$

$$s_{dk+1} - s_{dk} = i_{dk+1} - i_{dk} - \frac{u_{dk}^s + \omega_e L_q i_{qk}}{L_d} T_s \tag{14}$$

The control law is designed as

$$u_{dk} = \left[-q s_{dk} - \varepsilon \mathrm{sgn}(s_{dk})\right] L_d + u_{dk}^s \tag{15}$$

where $\varepsilon > 0$, $q > 0$, $1 - qT_s > 0$ and T_s is the sampling period.

For the q-axes, the sliding surfaces are designed as

$$\begin{cases} s_{qk} = i_{qk} - z_{qk} \\ \dfrac{z_{qk+1} - z_{qk}}{T_s} = \dfrac{u_{qk}^s - \omega_e L_d i_{dk} - \omega_e \psi_f}{L_q} \\ z_q(0) = 0 \end{cases} \tag{16}$$

The control law is designed as

$$u_{qk} = \left[-q s_{qk} - \varepsilon \mathrm{sgn}(s_{qk})\right] L_q + u_{qk}^s \tag{17}$$

Overall, for each axis, the controller output has two components: one are u_{dk}^s and u_{qk}^s and the other one are u_{dk} and u_{qk}. The u_{dk}^s and u_{qk}^s are designed for ideal system. Figure 5 shows the current regulator proposed in this paper, which is obtained by combining a direct discrete current regulator with a discrete sliding mode controller.

3.3. **Proof of robustness.** The switching function will be affected by the perturbation of parameters, external disturbances and other factors. So according to Equation (12), Equation (15) can be defined as following (18).

$$s_{dk+1} - s_{dk} = \frac{u_{dk} - u_{dk}^s - h_{dk}}{L_d} T_s \tag{18}$$

Select the Lyapunov function $v_k = s_k^2/2$, and the arrival conditions can be calculated as $s_{k+1}^2 < s_k^2$. When the sampling time T_s is small, it can get $2 - qT_s \gg 0$. The discrete sliding mode existence and arrival conditions can be described by the following equations:

$$[s_{k+1} - s_k]\mathrm{sgn}(s_k) < 0, \quad [s_{k+1} + s_k]\mathrm{sgn}(s_k) > 0$$

$$\begin{aligned}[s_{k+1} - s_k]\mathrm{sgn}(s_k) &= \left[-qT_s s_k - \varepsilon T_s \mathrm{sgn}(s_k) - \frac{h_{dk}}{L_d} T_s\right] \mathrm{sgn}(s_k) \\ &= -qT_s|s_k| - \frac{h_{dk}}{L_d} T_s \mathrm{sgn}(s_k) - \varepsilon T_s |s_k|\end{aligned} \tag{19}$$

$$\begin{aligned}[s_{k+1} + s_k]\mathrm{sgn}(s_k) &= \left[(2 - qT_s)s_k - \varepsilon T_s \mathrm{sgn}(s_k) - \frac{h_{dk}}{L_d} T_s\right] \mathrm{sgn}(s_k) \\ &= (2 - qT_s)|s_k| - \frac{h_{dk}}{L_d} T_s \mathrm{sgn}(S_k) - \varepsilon T_s |s_k|\end{aligned} \tag{20}$$

Equations (19) and (20) are established during $\varepsilon L_d > |h_d|$. And the sliding mode of the system is invariant for the parameter changes and the external disturbance. Thus, the robustness of the system can be proved. It can be certificated that the system is robust when the q-axis satisfies the inequality $\varepsilon L_q > |h_q|$.

4. Simulation Analysis and Experimental Verification.

4.1. Simulation analysis.

In order to verify the correctness of the proposed strategy, the simulation and experimental verification are carried out. The IPMSM parameters are shown in Table 1 which are measured in the ideal state. The system control block diagram is shown in Figure 6.

The curves (a) and (b) are a simulation curve based on the control strategy proposed in [8], and the target speed of curve (a) is 1500 r/min. The curves (c) and (d) are simulation waveforms when using a discrete current regulator based on the direct design method, and the curves (e) and (f) are simulation waveforms when using a current regulator based on discrete sliding mode compensation control. In the simulation experiment, the target

Table 1. IPMSM parameters

Parameters	Values
R_s	0.0126 Ω
L_d	280 μH
L_q	849 μH
ψ_f	0.116 Wb
T_e	60 N·m
Rated speed	4500 rpm
Pole	4 ploes

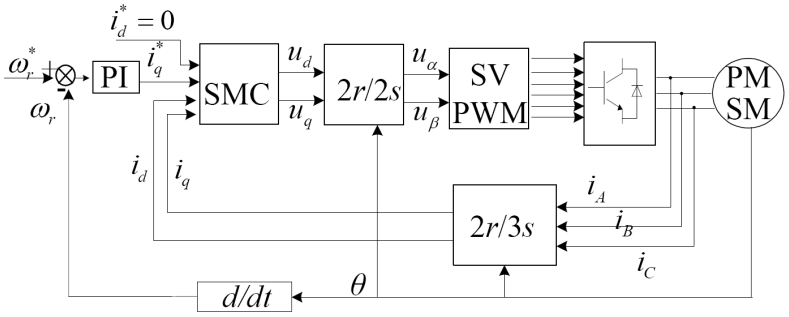

Figure 6. Block diagram of system

speed of IPMSM is 4000 r/min except the curve (a), and the initial load torque is 5 N·m. When $t = 0.15$ s, the load torque is stepped from 5 N·m to 15 N·m. The control strategy shown in Figure 6 is used in Figure 7, and then the two control algorithms are simulated under the exact and inaccurate parameters. The curves (c) and (e) are accurate for parameter identification, and curves (d) and (f) are $\hat{L}_{dq} = 1.3L_{dq}$. Compared with the curves (a) and (b), it can get a satisfactory decoupling effect on the low speed. However, on the high speed, as the previous analysis, there appeared high frequency noise and chattering phenomenon which will deteriorate the system's performance. So this method is not suitable for current decoupling control when in high speed. Compared with the curves (c) and (d) and the curves (e) and (f), it can be seen that the speed response and the decoupling effect of dq axis current are ideal for the same controller when the parameters are accurate. The dynamic performance of the current regulator is becoming worse when $\hat{L}_{dq} = 1.3L_{dq}$. If there is a sudden change in torque, the d-axis current also fluctuates. Contrasting curves (c) and (e) and curves (d) and (f) it can be got. For different controllers, when the parameter identification is accurate, the two control effects are similar. However, when the parameter identification is not accurate, the control effect proposed in this paper is much better than other control methods in the event of external disturbance.

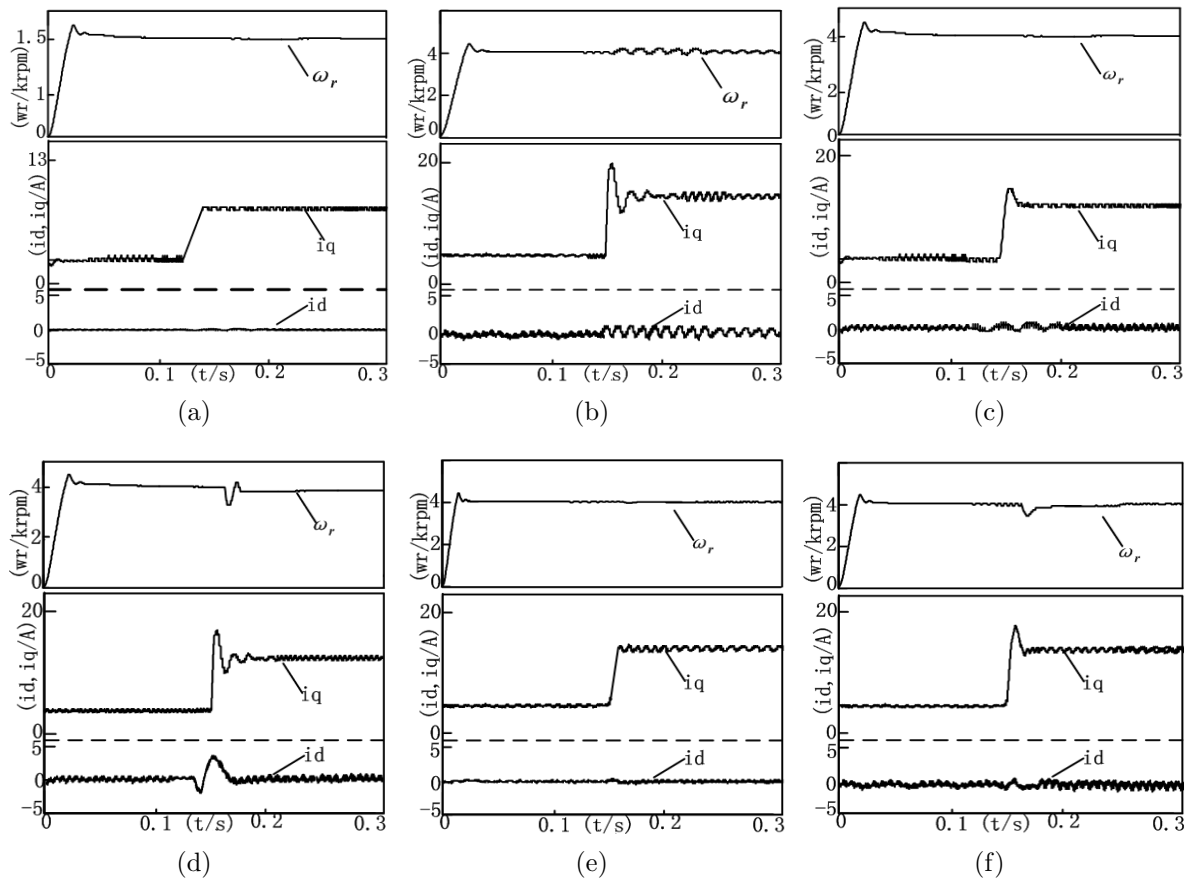

FIGURE 7. d/q axis current response for different discrete current regulators

4.2. **Experimental verification.** As shown in Figure 8, the motor test platform is built which is identical for the simulation model. The platform mainly includes the control module and the power module. The control module core control chip adopts TI's TMS320F28335. The power module includes FF600R07ME4 inverter and a series of detection circuits.

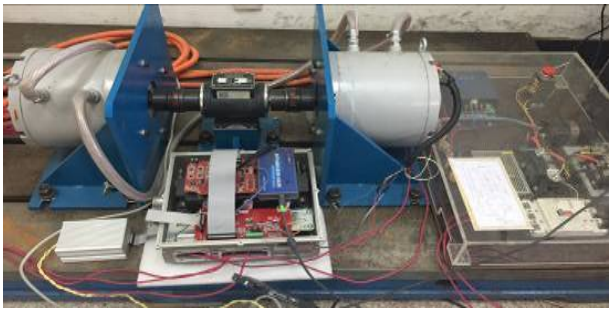

FIGURE 8. High-speed interior permanent magnet synchronous motor test bench

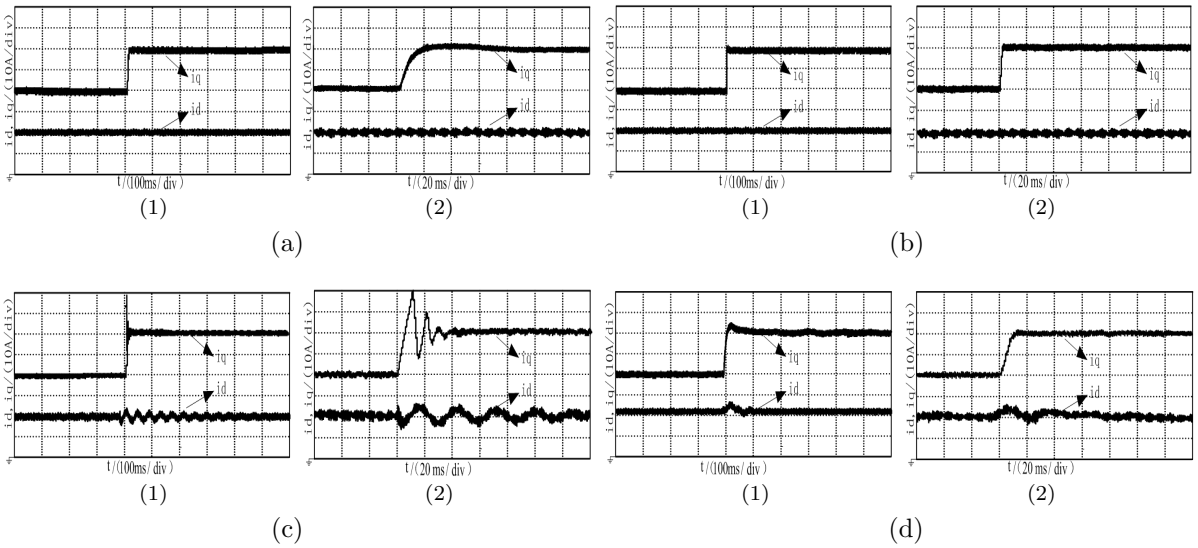

FIGURE 9. d/q axis current response for different current regulators

Figures 9(a) and 9(b) are the d- and q-axis current experimental waveforms for the exact motor parameters of the two controllers when the torque is mutation. Figures 9(c) and 9(d) are the d- and q-axis current experimental waveforms for the $\hat{L}_{dq} = 1.3L_{dq}$ of the two controllers when the torque is mutation, where (2) is a partial enlarged view of (1). Compared with (a) and (b), it can be seen that both methods can achieve better decoupling performance when parameters are accurate, and the second method is better than the first method in dynamic response. Compared with (c) and (d), it can be seen that when parameter is not accurate, the d- and q-axis of the first control method is cross-coupled seriously, and the d-axis current changes obviously when the q-axis current is mutation. The control method proposed in this paper can achieve ideal decoupling performance of current and the dynamic adjustment time is shorter than that of the first method. The system has strong robustness.

5. **Conclusion.** In this paper, a discrete sliding mode current compensation decoupling control is proposed, and it solves the problem that the traditional current controller decoupling effect is not ideal when there exist parameter changes or external disturbance for the system. According to the results of simulations and experiments, the proposed design improves the dynamic performance and robustness, particularly at high speeds, compared with the other methods. In addition, as we have seen, the current loop bandwidth is limited due to switching frequency and digital delay. In order to get the better performance under high speed for the control system, it will focus on expanding the current loop bandwidth in the future.

Acknowledgment. This work is partially supported by 'Hebei Science and Technology Department Project' and 'Hebei Province Higher Education Science and Technology Research Youth Fund Project'. We also gratefully acknowledge the helpful comments and suggestions of the reviewers, which have improved the presentation.

REFERENCES

[1] K. Wei, M. Zhou, Q. Zheng et al., Discrete-time current controller for induction motors based on complex vector, *Transactions of China Electro Technical Society*, vol.26, no.6, pp.88-93, 2011.

[2] H. Kim, M. W. Degner, J. M. Guerrero, F. Briz and R. D. Lorenz, Discrete-time current regulator design for AC machine drives, *IEEE Trans. Industry Applications*, vol.46, pp.1425-1435, 2010.

[3] A. G. Yepes, A. Vidal, J. Malvar, O. Lopez and J. Doval-Gandoy, Tuning method aimed at optimized settling time and overshoot for synchronous proportional-integral current control in electric machines, *IEEE Trans. Power Electron.*, vol.29, no.6, pp.3041-3054, 2014.

[4] M. Hinkkanen, H. A. A. Awan, Z. Qu, T. Tuovinen and F. Briz, Current control for synchronous motor drives: Direct discrete-time pole-placement design, *IEEE Trans. Industry Applications*, vol.52, no.2, pp.1530-1541, 2016.

[5] J.-S. Yim, S.-K. Sul, B.-H. Bae, N. R. Patel and S. Hiti, Modified current control schemes for high-performance permanent-magnet AC drives with low sampling to operating frequency ratio, *IEEE Trans. Industry Applications*, vol.45, no.2, pp.763-771, 2009.

[6] A. Altomare, A. Guagnano, F. Cupertino and D. Naso, Discrete-time control of high-speed salient machines, *IEEE Trans. Industry Applications*, vol.52, pp.293-301, 2016.

[7] G. Pellegrino, B. Boazzo and T. M. Jahns, Magnetic model self-identification for PM synchronous machine drives, *IEEE Trans. Industry Applications*, vol.51, no.3, pp.2246-2254, 2015.

[8] M. Comanescu, X. Longya and T. D. Batzel, Decoupled current control of sensorless induction-motor drives by integral sliding mode, *IEEE Trans. Industrial Electronics*, vol.55, no.11, pp.36-45, 2008.